

LA-UR - 77-206

CONFIDENTIAL

TITLE: ADVANCED LASER TECHNOLOGY FOR LASER-INDUCED FUSION APPLICATIONS

AUTHOR(S): Robert L. Carman

SUBMITTED TO: 4th International Workshop on Laser Interaction and Related Plasma, Plenum Press, New York, NY
Plenum Press, New York, NY

NOTICE
This report was prepared as an account of work sponsored by the United States Government of which the United States and the United States Energy Research and Development Administration, and its employees, and any of their contractors, subcontractors, or other employees, make no warranty, express or implied, or assumes any legal liability or responsibility for the accuracy or completeness of any information, apparatus, product, or process described, or represents that its use would not infringe privately owned rights.

By acceptance of this article for publication, the publisher recognizes the Government's (license) rights in any copyright and the Government and its authorized representatives have unrestricted right to reproduce in whole or in part said article under any copyright secured by the publisher.

The Los Alamos Scientific Laboratory requests that the publisher identify this article as work performed under the auspices of the USERDA.


Los Alamos
scientific laboratory
of the University of California
LOS ALAMOS, NEW MEXICO 87544

An Affirmative Action/Equal Opportunity Employer

DISTRIBUTION OF THIS DOCUMENT IS UNLIMITED

MSA 77-206

ADVANCED LASER TECHNOLOGY FOR LASER-INDUCED FUSION APPLICATIONS*

Robert L. Carman

University of California
Los Alamos Scientific Laboratory
Los Alamos, NM 87545

At least five years of committed work have already been spent on the development of very large laser systems, target geometries, and diagnostic capabilities. We will draw upon many significant features of this work to identify trends for future facilities. Also, because laser facilities are likely to be very much larger in the future, some additional conclusions seem unavoidable. As a stimulus for these discussions let us consider how we might design a 1-MJ laser facility today. This facility is large enough so as not to evoke many preconceived notions or biases, yet on the other hand, not too large to illustrate many of the problems we wish to point out. As an additional incentive for our review, let us recall, as demonstrated by many < 1 kJ target experiments (pulse duration 0.025 to 5 ns), that laser coupling inefficiencies as well as various undesirable energy-transport phenomena, for unsophisticated targets, dictate lasers with outputs of several hundred kilojoules to many megajoules to achieve significant net power generation (if not break-even) from laser-driven fusion. Current knowledge and laser research data clearly points to a number of weaknesses.

Let us first identify the crucial issues as follows:

1. Obtain complete flexibility and control of laser energy.
2. Design optimized amplifiers based on a deeper understanding of the processes involved, and
3. Increase laser efficiency.

Most of the discussion will deal with Item (2); Item (1) will be addressed in passing only, and Item (3) will be ignored.

* Paper presented at the 4th International Workshop on Laser Interaction and Related Plasma Phenomena, Troy, NY, November 8-12, 1976.

Control Of Laser Energy

The independent laser parameters which a laser designer has at his disposal are listed below:

TABLE I
INDEPENDENT LASER OUTPUT PARAMETERS

- (1) Total output energy.
- (2) Pulse duration (FWHM).
- (3) Output near-field spatial distribution and its time dependence.
- (4) State of polarization and its time dependence.
- (5) Temporal pulse shape.
- (6) Spatial distribution of focused output at target and its time dependence.
- (7) Wavelength at center of emission and its time dependence.
- (8) Instantaneous pulse-frequency bandwidth.

Several large analytic and numerical calculations have been performed to examine the effect of each of these parameters on laser-driven fusion, but experiments have concentrated mostly on items (1), (2), and (3) of Table I. Because small f-number optics are usually envisioned, use of only one polarization is excluded, and because only resonant absorption appears to have any polarization sensitivity of consequence, item (4) is usually considered to be best understood¹ and the least important. Almost from the beginning the last four items were assumed to be very important, but until recently little experimental work of significance has been carried out.

The capacity to temporally "Program" a laser pulse over several orders of magnitude in intensity has been developed, though little target work has been done. Two techniques exist: pulse stacking by means of beamsplitters² and electronic pulse programming combined with the electro-optic effect in Pockels cells.³ We at Los Alamos favor the latter because the former tends to maximize the peak power for a given pulse energy and total pulse duration (FWHM)

delivered to a target, leaving the additional time structure to drive undesirable plasma instabilities.

Uniformity of illumination at the target surface is usually accepted as desirable. However, direct focusing makes uniform target illumination by several beams, a very difficult task. This problem has been overcome by the development of confocal elliptical mirror systems.⁴ In fact when lasers with 20 or more output beams are employed, this problem should be simplified significantly, possibly eliminating the requirement for complex focusing optics.

We are thus left with the last two parameters of Table I, which have received little or no experimental attention until recently. A substantial number of target experiments have been carried out at $\lambda = 10 \mu\text{m}$ with CO_2 lasers and at $\lambda = 1 \mu\text{m}$ with Nd:glass lasers. One of the most important insights these experiments provided was the clear indication that the particle distributions divided into two portions: a hot component and a cooler background component. The background distribution does not appear to be substantially affected by laser wavelength⁵ and is characterized by a temperature of 0.3 to 1.0 keV. The hot distributions however are a different matter. Figure 1 plots the characterizing hot electron temperature, T_H , versus incident laser power⁶ for data obtained in labs across the world, as indicated. Although considerable data scatter exists for

Fig. 1.

Plot of characteristic hot electron temperature (for a two temperature model of the plasma) versus laser intensity on target. The upper curve is for CO_2 lasers while the lower is for Nd:glass lasers.

intensities, P_L , above 10^{15} W/cm² and interpretation of the data in terms of an electron temperature is often complicated by plateaus and other structure in the spectra, best-fit numbers have been used. Also included are some inferred hot-electron temperatures from maximum ion velocities observed in CO₂ thin-film experiments, assuming that the observed ions are accelerated in the isothermal corona of the laser plasma.

From Fig. 1 it is apparent that a single power law does not apply for all intensities. It is even more revealing to plot the data as a function of $P_L \lambda^2$, as in Fig. 2.⁶ Note that both the CO₂ and the Nd:glass data fall on one curve that evens out at about $P_L \lambda^2 = 10^{15}$ W·m²/cm². Particle-in-cell numerical simulations have shown that the laser drives up a steep density step. Such a step is due to the photon pressure exceeding the hydrodynamic plasma pressure and leads to a two-dimensional plasma surface which is unstable. Resultant turbulence, for large $P_L \lambda^2$ values, probably accounts for the larger scatter in the data. The solid curve drawn through the data above 10^{15} implies a $\lambda^{1/2}$ dependence from the indicated slope δ , and is the dependence found by particle-in-cell numerical simulations. The $\lambda^{4/3}$ scaling of T_{ij} for $P_L \lambda^2 < 10^{15}$ (weak profile-modification limit) is also as expected by the usual

Fig. 2.

Replot of data in Fig. 1 as a function of $P_L \lambda^2$ producing a universally applicable curve for both lasers.

flux-limit model. We believe that the reduction in power-law exponent is caused by laser modification of the density-gradient scale length to less than a free-space wavelength within the resonance-absorption model.⁶ These results indicate that any laser with only one time-independent center-emission wavelength λ and a relatively narrow linewidth, should lead to the same plasma properties under conditions of strong profile modification. To avoid the effect of strong profile modification while simultaneously improving inverse bremsstrahlung absorption, a laser wavelength of 0.3 μm is suggested. (Note that even at a laser intensity of 10^{16} W/cm², $P_L \lambda^2 = 10^{15}$.) However, there is one other aspect to be considered. A coherent laser of 0.3 μm wavelength has a 500 times higher capacity of producing interference-type structure in the focal plane than at 10.6 μm , whereas critical density of $\sim 10^{22}$ particles/cm³ implies that the critical surface is never too far from the solid target (density, $\sim 10^{23}$ particles/cm³). As a result, uniform initiation of the plasma is very improbable, because neither diffraction nor spatial thermal conduction can be expected to symmetrize the heating in such a short distance.

We know that ir lasers can generally initiate ablative compression quite symmetrically. On the other hand, uv lasers appear to be desirable in unsophisticated targets during the final portion of the ablative compression cycle, because strong profile modifications may be avoidable, losses in radial thermal conductivity are of lesser consequence, and inverse bremsstrahlung absorption is increased.

While sophisticated target design may eliminate these wavelength considerations, such targets are bound to be more expensive, making economical power generation less likely. Consequently, research designed to develop laser sources that can implode simple targets efficiently remains an important area for future research.

Let us consider the consequences of a totally different kind of laser source, namely one whose center wavelength jumps from the ir into the uv in several discrete steps. Such a laser could initiate plasma production in the ir at an intensity that would allow symmetry. By depositing the final laser energy in the uv at high intensity, improved inverse bremsstrahlung absorption and deposition of the laser energy at nearly solid density should ensure both good thermal and good optical coupling. By further providing several intermediate wavelengths, it also appears reasonable to expect a smooth transition that would avoid instabilities. Finally, if all this radiation were focused by a dispersive lens, a "spatial chirp" could be provided that would ensure a high focused intensity for the uv energy only.

Theoretical calculations have indicated that for normally included target physics significant benefits could be anticipated from this latter type of laser source. However, to our knowledge, only one proposal has suggested to date how such a laser source might be developed experimentally.⁷ This source involves an "after-

burner" concept of stimulated Raman scattering that takes place in a previously inverted medium. We will therefore, discuss more on this topic after having explored the more general subject of amplifiers.

DESIGN OF OPTIMIZED AMPLIFIERS

Let us consider the general requirements for a future amplifier system that will deliver 1 MJ in a pulse of 0.1 to 2 ns duration. We only assume that the amplifier medium stores the energy before amplification and that amplification involves the emission of one photon during the decay from the upper lasing level to the terminal level of the atomic or molecular system. We shall see that many aspects of the amplifier system follow from these simple assumptions and that the inclusion of practical limitations further defines the system.

First, consider the relation between total output energy W_{out} and beam diameter D dictated by practical limitations of the optical energy-flux F , namely,

$$D(\text{cm}) = \left(\frac{4W_{out}}{\pi M F} \right)^{1/2}, \quad (1)$$

where M is the number of parallel output beams, and whose cross sections have been assumed to be circular, for purposes of definitions. In fact any beam cross sectional shape is equally acceptable for present purposes, and a similar relation would result. Next, note that for steady-state pumping (i.e., for a condition in which an inversion is established, the energy is stored, and the pulse is amplified after most of the pumping cycle has been concluded), there are practical limitations on the diameter of the volume that can be excited by present pump sources, indicated in Table II. Present pumping sources seem to limit D to ~ 50 cm, within a factor-of-2 multiplier (numerator or denominator). Intensive research could certainly be expected to lead to a D much larger than 1.0 m within the next five years.

Note also that a practical flux limitation exists for any optical wavelength. It has been shown⁸ that for the whole infrared and low-frequency visible portion of the spectrum, an optical damage threshold exists for laser-beam windows, host material, and optical components in general at electric-field strengths very similar to the electric fields required for dielectric breakdown. A good upper flux limit for salt windows in CO_2 lasers ($10.6 \mu\text{m}$) is ~ 2 J/cm² at 1 ns, whereas, for iodine lasers ($1.3 \mu\text{m}$) or other potential gas lasers up to $\sim 0.3 \mu\text{m}$, sapphire windows are used, and can withstand up to 4 J/cm² at 1 ns, similar to ruby lasers. For uv excimer lasers, flux limits appear to be somewhat lower, 0.5 J/cm² for 1.0 - ns pulses dictated mainly by multiphoton absorption and related phenomena. While new materials may raise the flux limits somewhat, significant improvement seems unlikely. For any practical purpose we thus conclude that $F \sim 2$ J/cm², again good to a factor of

TABLE II

AMPLIFIER DIAMETER CONSTRAINTS FOR STEADY STATE PUMPING

- I. FLASHLAMPS (CONVENTIONAL OR SCINTILLATORS)
Diameter-density of absorber constraint imposed due to inversion uniformity. Typically $D < 50$ cm for reasonable N^* .
- II. SUSTAINER OR CONVENTIONAL DISCHARGE
Diameter constraint due to loss of E/P at large gaps stemming from streamer and breakdown problems. Typically $D < 50$ cm for reasonable pressures.
- III. ELECTRON BEAM
Voltage scales with pressure (new area). For typical pressures, a 50 cm square cross section requires a megamp (leading to current pinch effects). With use of magnetic fields, might scale to one meter square cross section.
- IV. CHEMICAL
Gas mixing to reasonable homogeneity limit pure chemical system to $D \ll 50$ cm. A premixed initiated chemical system is limited by initiator unless it's a chain reaction. True chain reaction is not a steady-state pumping situation.
- V. NEUTRON, X-RAY, OR OTHER BEAMS
Scaling conceptually feasible to large sizes but very little known. If fissionable materials included, pumping may not be steady-state.

2. From Eq. (1), we see that for an output $W_{\text{out}} = 1 \text{ MJ}$, 250 beams are required and each with a diameter of 50 cm. While there is hope that research might increase D substantially, we are still led to the conclusion that we must develop means to combine groups of beams into clusters and then treat them as one entity. We will define an array as such a cluster of beams which, once generated, is then manipulated, expanded, split, amplified, focused and isolated as if it were one beam. A laser system consisting of many parallel arrays of beams is then termed an array laser.⁹ Future large facilities may even proceed to arraying several arrays as indicated in Fig. 3. Note that the top left (Fig. 3) represents schematically the array to be used in the 100-kJ High Energy Gas Laser Facility (HEGLF) to be constructed at Los Alamos. Six parallel amplifiers with 12 segments per amplifier are envisioned. The middle left array of Fig. 3 was first proposed by the author at Lawrence Livermore Laboratory in 1972.⁹ Such arrays can be further combined at a later stage into arrays of arrays as a generalization of the illustration in the upper right of Fig. 3. In Fig. 4, we show the near-field pattern of an actual laser output, illustrating one method of generating a beam array. This array consists of 155 independent but collinear beams, which were generated by a ruby oscillator consisting of a uniformly inverted 25-mm-diam. rod of 25 cm length, a 10% reflecting output mirror, a fully reflecting rear mirror, a saturable-absorber Q-switch, and an aperture plate placed near the rear mirror. The aperture plate is perforated by a series of 1-mm-diam. holes, arranged as shown by the optical pattern in Fig. 4. By operating this system as a driven or regenerative amplifier rather than as an oscillator, it would be further possible to guarantee that all beams were time-synchronized. In fact, even complete phase synchronization might be attainable with this approach.¹⁰

An alternative approach first conceived by Gene McCall and the author in 1975 in Los Alamos is shown in Fig. 5. In this case, a beam entering from the left is split twenty times by partial transmitting mirrors located in the optical path. Beam collinearity is then reestablished by 20 totally reflecting mirrors located at the perimeter of a very stable, water-cooled, stainless steel frame. The locus of the emerging beams is a circle with its center on the original beam axis. As shown schematically the 20 beams then traverse an amplifier stage on the extreme right. Array lasers simply cannot be avoided in future laser systems unless great breakthroughs occur in laser pumping. Professor Basov's 216-beam and Professor Prokhorov's 52-beam Nd:glass lasers and the 6 segmented-donut beams of the Los Alamos CO_2 100-kJ laser, are employing to some extent these ideas although probably for different reasons.

From our preceding discussion much more can be inferred, however, than just the number of beams. We know as an empirical fact that a limit exists for the product of gain coefficient g and amplifier diameter D namely,

Fig. 3.

Beam cross sectional profiles of possible interest for array lasers, showing the clustering of several smaller beams into a large "beam".

Fig. 4.

Cross sectional beam profile consisting of 153 beams of 1 mm diam.
generated by a 25 mm diam. ruby oscillator.

Fig. 5.

Illustration of a beamsplitter (left) capable of producing a beam array of 20 collinear beams from one input beam, and an array amplifier (right) capable of amplifying all 20 beams as if they were one beam.

$$g_{\max} (\text{cm}^{-1}) = (\sigma N^*)_{\max} < 5/l \approx \left[\frac{6\pi M F}{W_{\text{out}}} \right]^{1/2} \quad (2)$$

Equation 2 frequently does not arise due to a limited amplified spontaneous emission but from several other limitations; to date, a more typical value of $g_{\max} l \leq 2$ is observed. From Eq. (2) we can immediately find the energy storage density, E_s , again to within a factor of 2, because essentially the whole output must be stored in the last amplifier gain length. Therefore,

$$E_s (\text{J/cm}^3) = F g < F^{3/2} \left[\frac{6\pi M}{W_{\text{out}}} \right]^{1/2} \quad (3)$$

This relationship also implies that for a simple transition the saturation energy flux equals the flux limit F . The required inversion density can now be established, if the laser wavelength is specified, namely

$$N^* (1/\text{cm}^3) = \frac{E_s \lambda (\mu\text{m})}{2 \times 10^{-19}} < \frac{F^{3/2} \lambda (\mu\text{m})}{2 \times 10^{-19}} \left[\frac{6\pi M}{W_{\text{out}}} \right]^{1/2} \quad (4)$$

Finally, combining the equalities of Eqs. (3) and (4), we see that

$$\sigma_{\text{opt}} (\text{cm}^2) = g/N^* = \frac{2 \times 10^{-19}}{F \lambda (\mu\text{m})} \quad (5)$$

This relation provides us with the optimum emission cross section σ_{opt} for the amplifying medium of a large laser. Because most lasers do not operate with this cross section, let us ask what the consequences are. For $\sigma < \sigma_{\text{opt}}$, the beam saturation-energy density in the amplifier is higher than the flux limit F , implying that energy extraction is incomplete and hence inefficient, as in the case of glass lasers. On the other hand, for $\sigma \gg \sigma_{\text{opt}}$, amplifier saturation occurs early in the pulse-amplification process, as is the case in CO_2 lasers, and very large volumes of inverted media are required due to linear rather than exponential spatial gain, so that hardware costs are much higher than they are for a truly optimum system. Of all the lasers currently considered for obtaining > 1 -kJ pulses of ≤ 1 ns duration, only atomic iodine can achieve this optimum emission cross section. In experiments at Los Alamos, we have broadened the iodine line with 1 atm of Xenon mixed with 100 torr of CF_3I , which upon flashlamp photolysis, yields 10 torr of inverted atomic iodine with a cross section $\sigma = 2 \times 10^{-19} \text{ cm}^2$ in a 1-cm-diam. tube. Further, the atomic-iodine laser of Zeuv and Basov at the Lebedev Institute in Moscow closely approaches this cross section in an exploding-wire-pumped 50-cm-diam. amplifier, indicating that only efficiency questions associated with the pump source may provide some limitations on atomic-iodine lasers. The three most prominent laser systems in use today are compared in

Table III. We have introduced two new parameters in this table. The first is

$$\ell_{\text{characteristic}} = \frac{1}{100g} \ln \left[\frac{10^9}{LM} \right], \quad (6)$$

where g is the exponential gain coefficient. In arriving at Eq. (6), we assume unsaturated gain as well as 1-MJ output from an amplifier chain of L times M beams driven by a 10^{-5} -J oscillator input. The last table entry is the product of the three preceding entries and is proportional to the total volume of the amplifier system. In the case of CO_2 , the early saturation of the amplifier chain will lead to a somewhat greater length. While all three systems could be scaled to 1 MJ, the $\text{I}^*\text{-Xe}$ laser clearly should be least expensive because it should involve only 1/6th the volume of inverted material needed in CO_2 lasers; however, due to its presently much lower efficiency than that of CO_2 lasers, much or all of this advantage is not realized.

TABLE III

ONE MEGAJOULE ARRAY LASERS FROM PRESENT LASER MEDIA

	<u>Nd:Glass</u>	<u>I*-Xe</u>	<u>CO*-He</u>
$\sigma(\text{cm}^2)$	3×10^{-20}	2×10^{-19} (1 atm)	6×10^{-19}
$N(\text{J}/\text{cm}^3)$	10^{18}	2×10^{17}	4×10^{16}
$g(\text{cm}^{-1})$.03	.04	.025
$D(\text{cm})$	30	50	35
$F(\text{J}/\text{cm}^2)$	2	4	2
$E_s(\text{J}/\ell)$	190	30	.8
L Paths	35	25	44
M Beams/Path	20	5	12
$\ell_{\text{Characteristic}}(\text{m})$	4.7	4.0	5.8 [#]
L M ℓ_{CIAR}	3290	500	3060 [#]

[#]Since amplifiers operate highly saturated this number is not correct, but rather should be somewhat larger.

We now turn to concepts that may alter some of the details thus far presented. The solid curve in Fig. 6 plots the laser emission cross section versus energy output per beam over a wide range of values.¹¹ Also indicated are the relative expected output energies under steady-state pumping conditions for several different laser systems. Finally, we show by what techniques these output energies might be increased. In the remainder of this paper, we will explore these techniques.

Fig. 6.

Plot of laser emission cross section versus relative energy output/beam used to divide space into three identifiable regions. Conventional lasers with both steady state pumping and single photon energy extraction operate at best on the plotted curve or to the left of the curve.

First, let us explore the concept of transient amplifier inversion, i.e., a situation in which the duration of the pump pulse is comparable to the laser output pulse in the amplifiers, while the oscillator is a quasi-cw source (on the scale of the amplifier pumping pulse). One good example of this type of laser system is an HF laser.¹²

One advantage of transient inversion is the possibility of eliminating superfluorescence problems if the cw laser input power greatly exceeds the optical-noise power, implying that any large cross section σ is usable because energy storage is no longer required. Further, it should be possible (within uncertainty-principle constraints) to preserve the input frequency and the spatial optical distributions of the quasi-cw input source. Because energy storage is not required, the amplification process could be carried out in a medium in which each active atom or molecule is used many times in the pumping-energy extraction process, implying that the total density of the active medium could be much reduced. Finally, chain-reaction processes appear to make devices of much larger aperture possible, suggesting that substantially fewer beams than presently considered are required for very large laser systems.

The disadvantages of transient pumping are quite significant, however. The pumping power required for amplifier inversion is comparable to the laser output power indicating that we are dealing only with an improvement in the Q of the energy, where Q is the center frequency of the energy source divided by the frequency bandwidth of the source. Further, medium homogeneity must be adequate to preserve the spatial intensity distribution of the initial input. Finally, control of the temporal distribution of the amplifier output demands that the temporal distribution of the pump be controlled, and this will certainly be very difficult.

Presently we are attempting to evaluate these systems in a very small and simple experimental setup consisting of a laser-pumped dye oscillator/amplifier system in which the two laser pumping sources are of a different and programmable duration and pulse shape. The dye-laser oscillator produces an output pulse of ~ 100 ns duration, 0.01 cm^{-1} bandwidth, 2 mm diameter, and ~ 10 mJ energy. The dye-laser amplifier has a pumped volume 2 mm in diameter by 1 cm long and a pumping duration of ~ 1 ns in a transverse excitation geometry. Experiments using longitudinal pumping are being considered. Typical gains of 60 db/cm have been observed, suggesting that many of the questions associated with energy extraction can be answered with this system.

In a second transient-inversion study we are using the tunable dye-laser oscillator described above as an input idler in a traveling-wave-pumped parametric amplifier. A LiNbO_3 crystal, 25 mm in diameter by 4.5 cm long, is available; we intend to use again the 1-ns ruby laser pump for this experiment. Because both the dye oscillator and the ruby pump have bandwidths of ~ 0.02 cm^{-1} , we expect a very narrow bandwidth for both the new parametric amplifier

output and the amplification on the idler.

While neither of these systems is expected to lead directly to a very large laser, we hope to model the problems associated with such systems so as to evaluate their prospects. We expect that the low Q-high power pump source for a final system will be either chemical, nuclear, or thermal.

The lower right-hand corner of Fig. 6 points up one other possibility, namely amplifiers involving multiple-photon energy extraction. In these systems energy storage and energy extraction are separate phenomena, which as indicated, is most relevant to lasing media with very low emission cross sections. In principle, we can produce an amplifier in which the small-signal gain at all frequencies is much lower than the large-signal gain for the input driving laser. It is almost correct to state for these amplifiers that their normal emission cross section σ is replaced by $\sigma_{NL} \cdot I$, where I is the intensity of the driving laser.

The advantages of this type of amplifier are numerous. First, we might expect large energy-storage densities without losses due to superfluorescence. Also, because the gain depends on driving-laser intensity, we expect temporal narrowing of the amplified pulse due to the amplifier's nonlinear response. Finally, we have the possibility of changing the frequency of the driver pulse during amplification if we choose the nonlinear system properly. In fact, through the use of stimulated Raman scattering, we can provide a uv frequency chirp on the amplified pulse which should lead to an output pulse bandwidth of many tens of thousands of inverse centimeters.

The disadvantages of this type of amplifier are, however, formidable. First, stimulated two-photon emission (Process A of Fig. 7) has not been observed experimentally, a fact that might be rectified in the near future. Also, the state of the art in laser technology coupled with large non-radiative loss rates limit currently available energy-storage densities to marginally interesting values. Further, the output-flux limits that had been discussed earlier also apply to nonlinear amplifiers, and moderately large nonlinear emission cross sections imply that only limited energy gains are possible. We should pursue this option because advantages promise to be great and because none of the disadvantages seem to involve fundamental problems.

Two nonlinear amplification schemes are indicated in Fig. 7. Process A corresponds to two-photon emission (TPE), whereas process B corresponds to stimulated Raman scattering (SRS) in an inverted medium, sometimes also referred to as anti-Stokes Raman scattering (ASRS). As discussed in reference 7, process A becomes most probable when $\omega_1 = \omega_2$, and this condition is referred to as degenerate two-photon emission (DTPE).

The principal difference between TPE and SRS is caused by the fact that photon number conservation limits energy gain to ω_3/ω_1 , whereas no such conservation law exists for TPE. However, because

Fig. 7.

Energy level diagram illustrating two nonlinear amplification processes. A) Two-photon stimulated emission, B) anti-Stokes stimulated Raman scattering.

ω_3 can act as the input wave for further SRS, leading to the generation of $\omega_5 = \omega_3 + \omega_2 + \omega_1$ and so on, moderate energy gains are feasible even for SRS. Specifics for a practical case are given in Fig. 3 of Ref. 7. To calculate the maximum energy gain achievable for all orders of ASRS, we only need to calculate the last output frequency expected:

$$\omega_{(2n+2)} = \omega_2 + 2n (\omega_1 + \omega_2) \text{ where } n \text{ is the order of SRS, and } G_{\max} = \omega_{2n+2}/\omega_2.$$

Two kinds of spectroscopy are of interest for the amplifying media, as illustrated in Fig. 8 for atomic iodine and atomic oxygen. For atomic iodine, we desire DTPA initially to give way to ASRS, which should proceed for many orders. Note that $\omega_3 = 3\omega_1$ i.e., stimulated third-harmonic generation, which is enhanced by the para-

Fig. 8.

The atomic energy levels pertinent to nonlinear amplification. Also included are indicators of the energy extraction process suggested by the spectroscopy.

metric production of third harmonics in the presence of a resonant two-photon level. Further, because $\omega_5 = 5\omega_1$ this device is an odd-harmonic generator with gain. Atomic iodine is a particularly good choice, not only because ω_1 lies in the ir, namely at $\lambda = 2.65 \mu\text{m}$, but also because no cancellation from the intermediate states occurs in the odd-harmonic response up to about the 13th harmonic, due to the isolated two-level nature of the spectroscopy. As a final benefit, as we proceed from the third harmonic to the fifth, the seventh, and so on, the levels become more and more resonant with the intermediate states, implying that the gain of the higher odd harmonics is increasing, thus forcing the energy of each new harmonic to exceed that of the preceding one. Also note that, $2.65 \mu\text{m}$ is the fourth harmonic of the normal CO_2 laser operating at $10.52 \mu\text{m}$. We thus might envision a large CO_2 laser whose output first passes through two sequences of second-harmonic generators and then through an inverted atomic-iodine cell before being focused on target. As the $10.52 \mu\text{m}$ output increases, a wavelength of $5.26 \mu\text{m}$ reaches the target followed by $2.65 \mu\text{m}$; then the iodine cell amplifies the $2.65 \mu\text{m}$ output, followed by odd-harmonic generation to $0.877 \mu\text{m}$, then $0.526 \mu\text{m}$, then $0.376 \mu\text{m}$, then possibly $0.292 \mu\text{m}$, and so on, with the intensity increasing with frequency and the highest frequency generated being determined by either absorption of one or two photons, or by optical breakdown of the medium by the previous harmonics.

Numerical simulations of an atomic-iodine nonlinear amplifier have confirmed the properties discussed above, and energy gain of up to 100 have been achieved for an input intensity of $5 \times 10^8 \text{ W/cm}^2$ at $2.65 \mu\text{m}$. However, one other problem has been revealed by the numerical work. The nonlinearity of the gain creates a spatial instability because the gain is highest where the intensity is highest. We thus find that a flat-topped spatial distribution is required for the input laser, very similar to that generated in highly saturated amplifiers, like those typically employed in a large CO_2 laser systems. The nonlinear system described above could provide a center-frequency change from $10.5 \mu\text{m}$ to at least $0.376 \mu\text{m}$, corresponding to a 28-fold change. If two-photon absorption stops the amplification, only harmonics up to the seventh will be produced in the iodine. On the other hand, if single-photon absorption stops the process, we might expect two or even three additional odd harmonics, namely 0.292 , 0.239 , and possible $0.202 \mu\text{m}$, thus providing another two-fold change in frequency. The use of these latter frequencies, however, will be greatly complicated by transmission difficulties in air, windows, and optical components.

Further confirmation of this Raman behavior was found in a thesis by G. Kachen¹⁵ who studied normal Raman scattering in gases at 1.1 μ by using the second harmonic of a Nd:glass 1-ns laser system and a 5-ps-resolution streak camera. Some typical time resolved spectra taken from this work are shown in Fig. 9. For SF_6 , $\omega_R = 774 \text{ cm}^{-1}$, whereas for N_2O , $\omega_R = 1282 \text{ cm}^{-1}$ and for Cl_4 , $\omega_R = 2916 \text{ cm}^{-1}$

Fig. 9.

Streak camera records of the time dependence of stimulated Raman scattering performed in the high pressure gases under conditions of steady state (upper) and transient (lower) response.

in the case of SRS.¹⁴ Finally, for H_2 , $\omega_R = 4155 \text{ cm}^{-1}$. In the first three cases, the SRS is operating in a steady-state condition,¹⁵ whereas for H_2 the SRS is transient.¹⁵ Notice that for SF_6 the higher orders are generated as expected, but that regeneration of prior orders also occurs. Because of the small frequency shift and the very small dispersion in SF_6 ,¹⁶ anti-Stokes/Stokes coupling through the phase-matched four-photon interaction leads to this regeneration. Less regeneration occurs for the more dispersive cases of N_2O and CH_4 . Finally, in the case of transient SRS, very little regeneration is to be expected and none was observed in the case of H_2 , providing additional corroboration. In the case of inverted atomic iodine, $\omega_R = 7605 \text{ cm}^{-1}$; because the gas is very dispersive little or no regeneration of prior orders should occur.

We are presently experimenting to evaluate the resultant quasi-white light source by using inverted atomic iodine and a 2.63- μm driving laser source. The experimental setup is shown schematically in Fig. 10. Previously, we demonstrated ASRS in inverted atomic iodine, obtained through flashlamp photolysis, and a Nd:glass driving laser system of $\sim 1 \text{ ns}$ pulse duration.¹⁷ In our present experiment we are using a two-pulse ruby laser to pump, first, a well mode-selected-dye oscillator-amplifier system as well as a traveling-wave LiNbO_3 parametric amplifier (see Fig. 10). This source is in the final stages of development and should produce a 2.63- μm beam of $\sim 1 \text{ ns}$ duration with an intensity of up to 2.5 GW/cm^2 . Two stages of an improved iodine system, used in previous work,¹⁷ then provide nonlinear amplification. In this experiment, we expect a pulse-energy gain of ~ 10 and only few odd harmonics because the cell containing the medium is a little too short. We also expect to study DTPE and its competition with ASRS.

The other type of DTPE device of interest requires an atomic spectroscopy like that of Fig. 8 for atomic oxygen. Here, we attempt to eliminate ASRS completely by placing the intermediate state about halfway between the upper and the lower two-photon laser states. Further, only circularly polarized light would be employed to prevent parametric third-harmonic generation. Finally, we should look for an absorber gas that would absorb the third harmonic if ASRS does occur. As a consequence we would only use the two-photon emission mode. In the case of atomic oxygen, we expect gain at $\lambda = 0.592 \mu\text{m}$ between the $\text{O}(^1\text{S})$ and the $\text{O}(^3\text{P})$ levels with $\text{O}(^1\text{D})$ representing the near-resonant intermediate state. Estimates of the expected two-photon emission cross section for atomic oxygen suggest that it should be within one order of magnitude of that expected for atomic iodine.⁷ Finally, the single photon emission cross section for the decay of $\text{O}(^1\text{S})$ to $\text{O}(^1\text{D})$ is sufficiently small to allow a substantial inversion to be obtained.

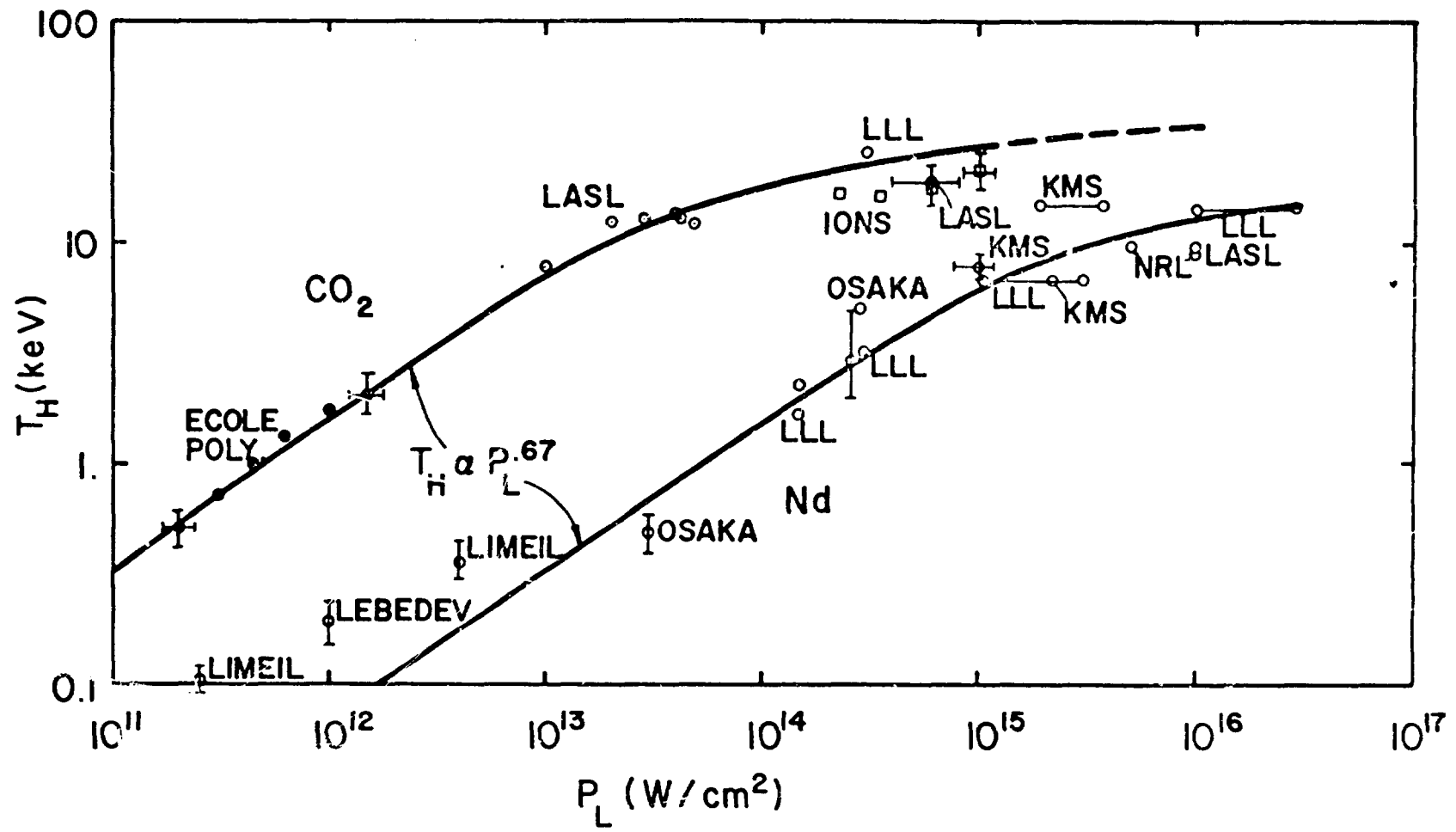
Fig. 10.

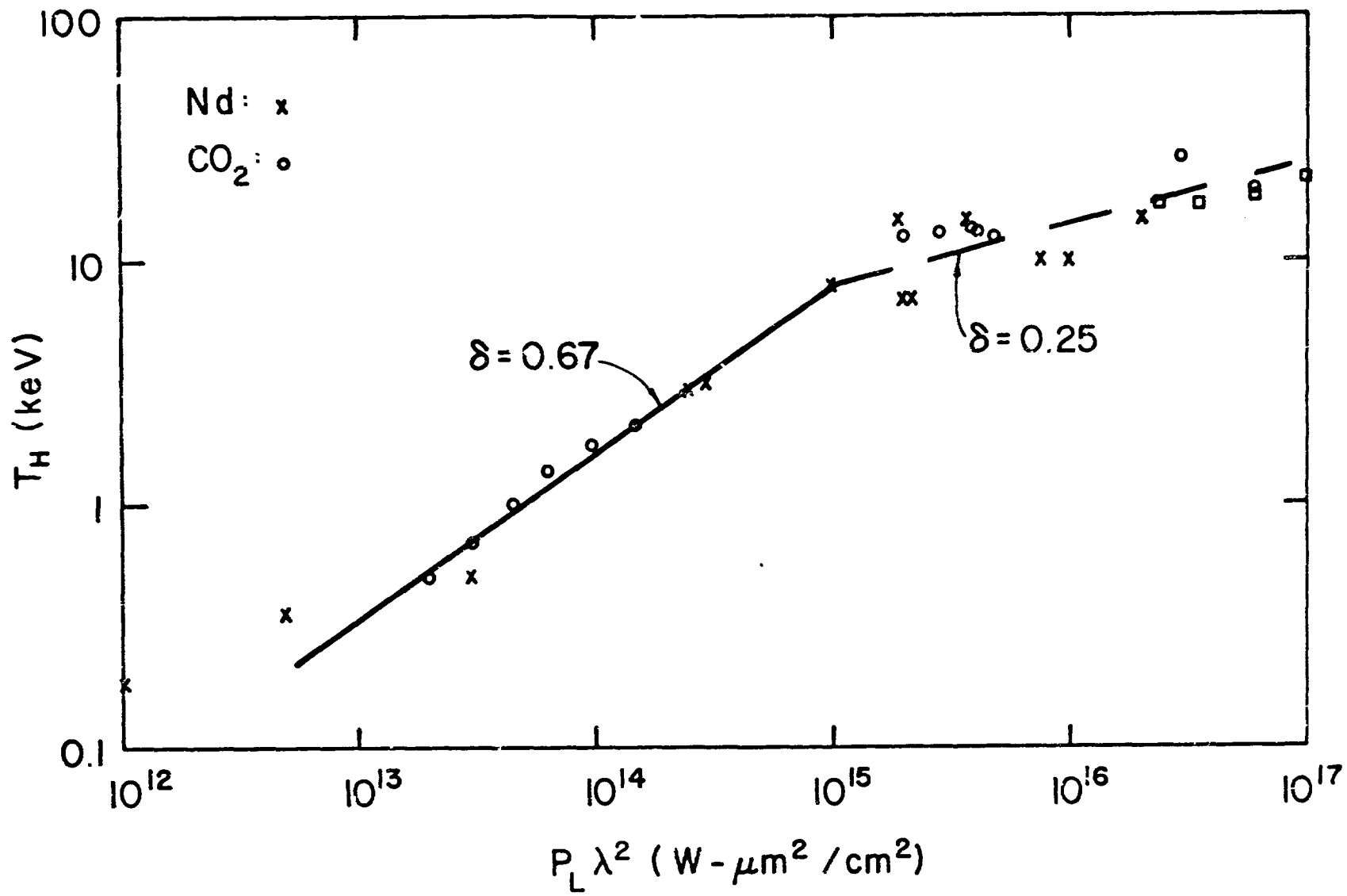
Schematic of experiment to demonstrate both degenerate stimulated two-photon emission and odd-harmonic generation with exponential gain through stimulated Raman scattering in inverted atomic iodine.

REFERENCES

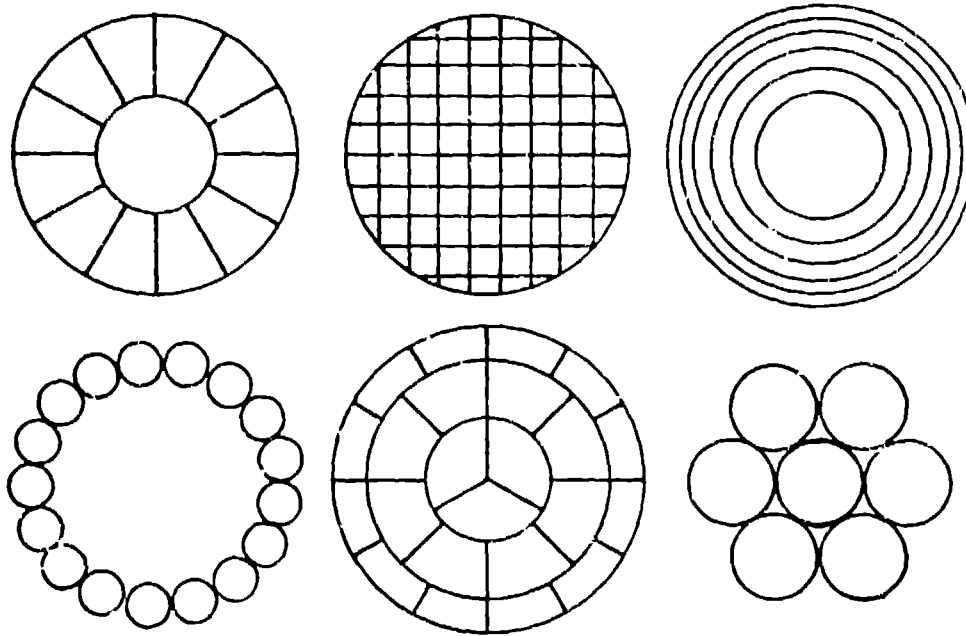
1. See, for example, P. Kolodner and E. Yablonovitch, Phys. Rev. Letters 57, 1754 (1976), J. Pearlman, Sandia Laboratories, private communication.
2. This idea was first proposed at KMS Industries and now precise equipment is available commercially from Quantel International. See paper in this conference by G. Bret.
3. See paper presented in this conference by R. L. Carman, A. G. Engelhardt, and N. Glabo. Also, see R. L. Carman, "Optical Pulse Programming for Laser Fusion," Conference on Lasers and Nonlinear Optics, Tbilisi, USSR (1976); and Los Alamos Scientific Laboratory Report, LA-UR-76-1015 (1976), R. L. Carman Bull. Am. Phys. Soc. 20, 1286 (1975).
4. C. E. Thomas, Appl. Optics 14, 1267 (1975).
5. See D. J. Nagel, Bull. Am. Phys. Soc. 21, 1120 (1976) and reference therein.
6. Figures by D. V. Giovanielli; see D. V. Giovanielli, "Wavelength Effects in Laser Fusion," Los Alamos Scientific Report, LA-UR-76-2242 (Rev. 1), (1976) and Bull. Am. Phys. Soc. 21, 1047 (1976); see also D. W. Forslund, J. M. Kindel and K. Lee, Phys. Rev. Letters (to be published), and *ibid*, Los Alamos Scientific Laboratory Report, LA-UR-77-29 (1977).
7. R. L. Carman, Phys. Rev. A 12, 1048 (1975).
8. E. Yablonovitch and N. Bloembergen, Phys. Rev. Letters 29, 907 (1972); E. Yablonovitch, Appl. Phys. Letters 25, 121 (1975).
9. First reported by R. L. Carman, "Current Laser Technology and Understanding and Proposed Big Laser Machines," Lawrence Livermore Laboratory, Internal Memorandum (1975).
10. R. L. Carman, "Array Laser - A Technique for the Generation of Ultra-High Laser Intensities," Los Alamos Scientific Laboratory Report, LA-UR-75-2260 (1975).
11. R. L. Carman and C. K. Rhodes, work in progress.
12. R. W. Getsinger, R. N. Greiner, K. D. Ware, J. P. Carpenter, and R. G. Wenzel, "Controlled Energy Extraction and Sharp Nanosecond pulses From an HF Amplifier," Los Alamos Scientific Laboratory Report, LA-UR-76-1020 (1976); R. W. Getsinger, D. K. Ware, J. P. Carpenter, "Generation and Amplification of Nanosecond Duration, Multiline, HF Laser Pulses," Los Alamos Scientific Laboratory Report, LA-UR-76-1444 (1976).
13. G. Kachen, University of California, Davis, Livermore Extension, thesis (1974), unpublished.

14. M. E. Mack, R. L. Carman, J. Reintjes, and N. Bloembergen, Appl. Phys. Letters 12, 209 (1970).
15. R. L. Carman, F. Shimizu, N. Bloembergen, and C. S. Wang, Phys. Rev. A2, 60 (1970).
16. R. L. Carman and M. E. Mack, Phys. Rev. A5, 541 (1972).
17. R. L. Carman and W. H. Lowdermilk, Phys. Rev. Letters 53, 190 (1974).

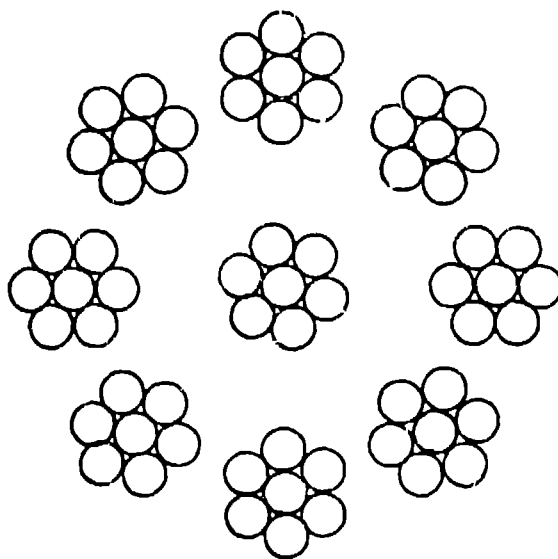


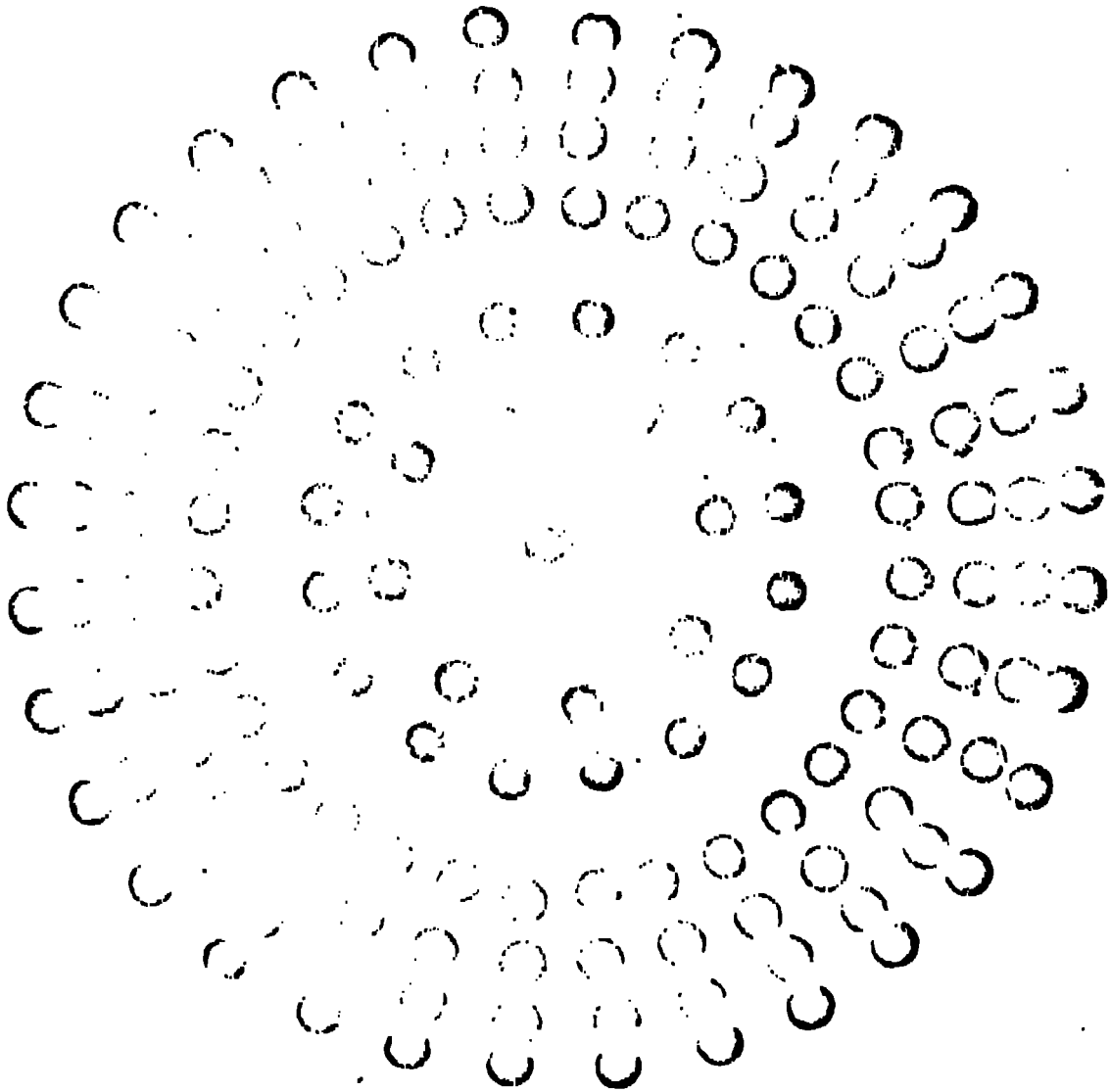


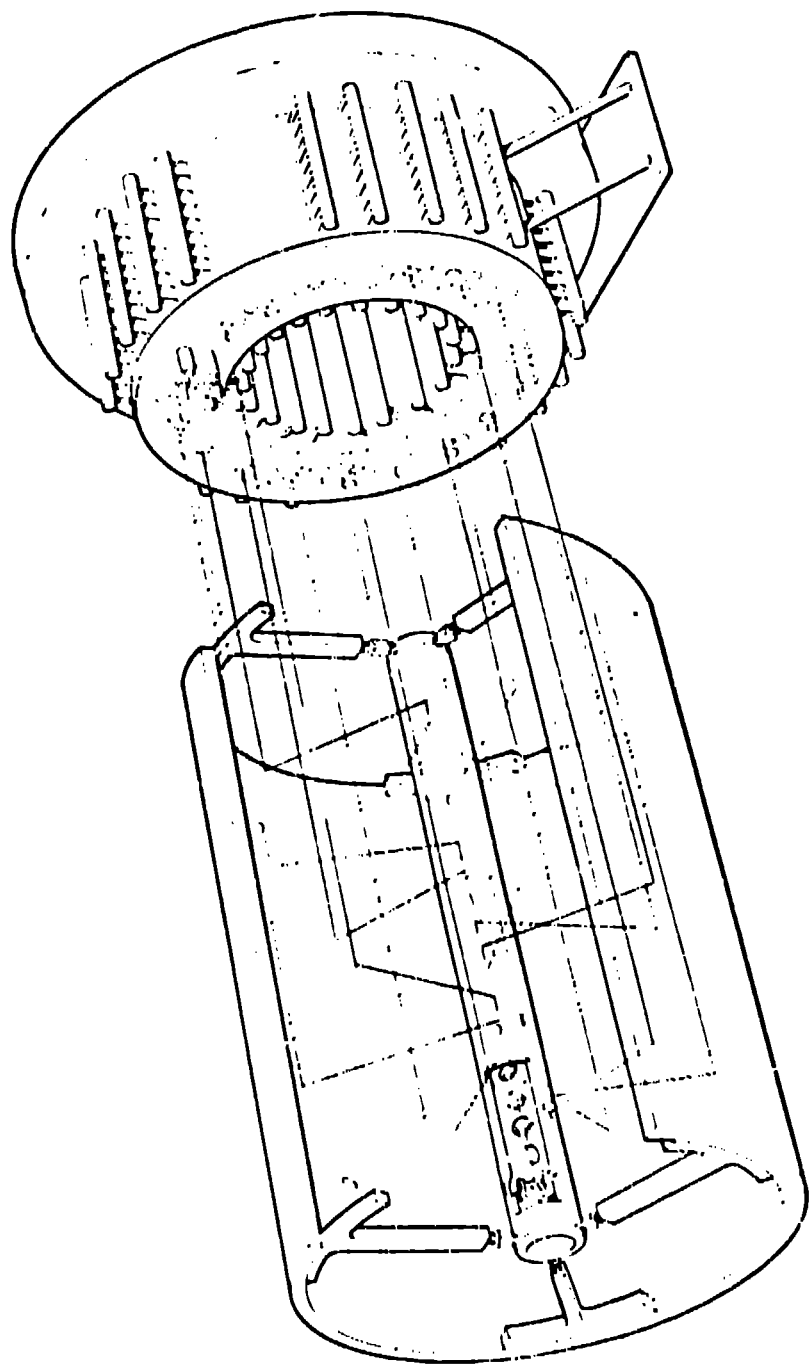
EXAMPLES OF LASER BEAM ARRAYS

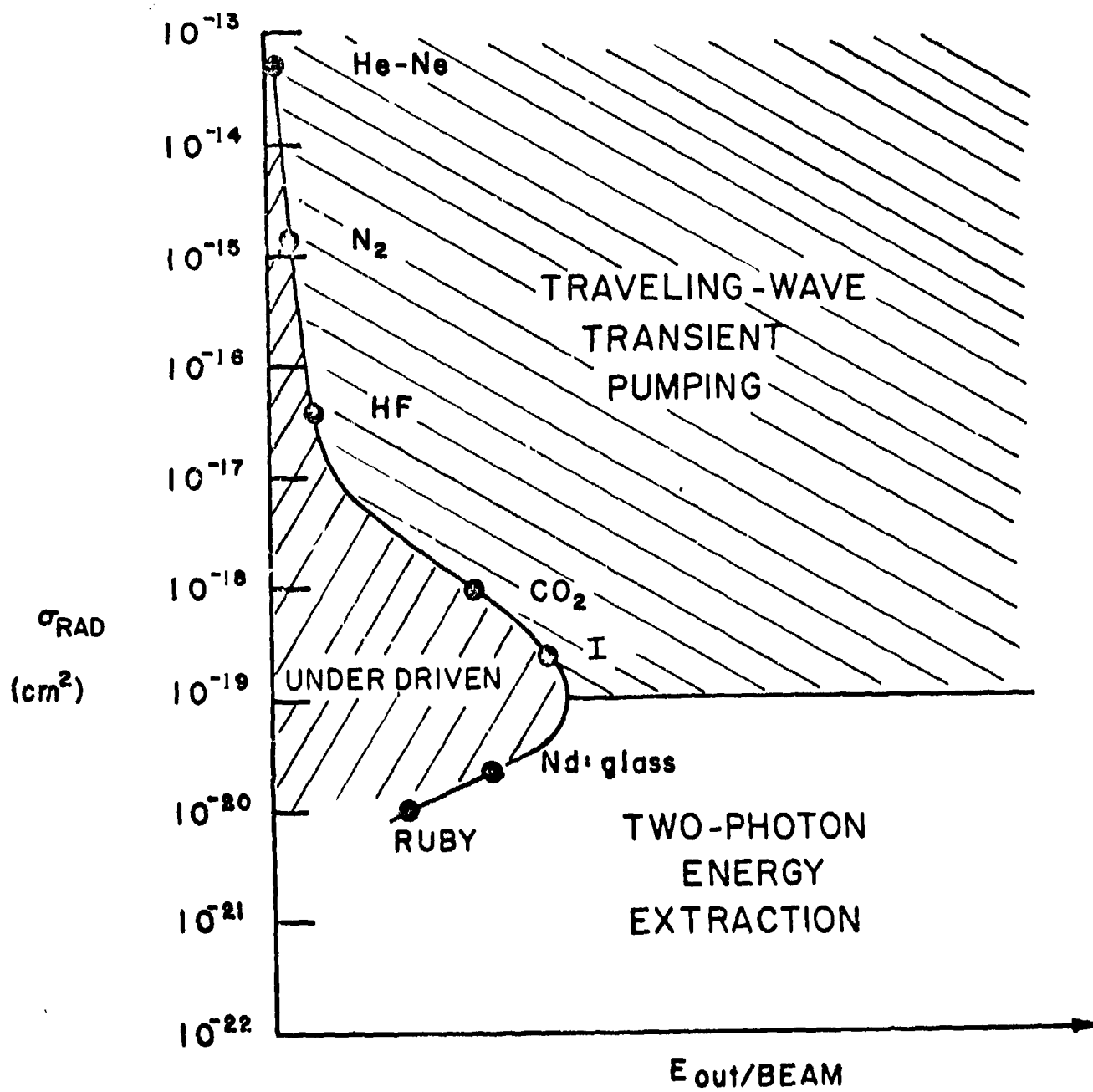


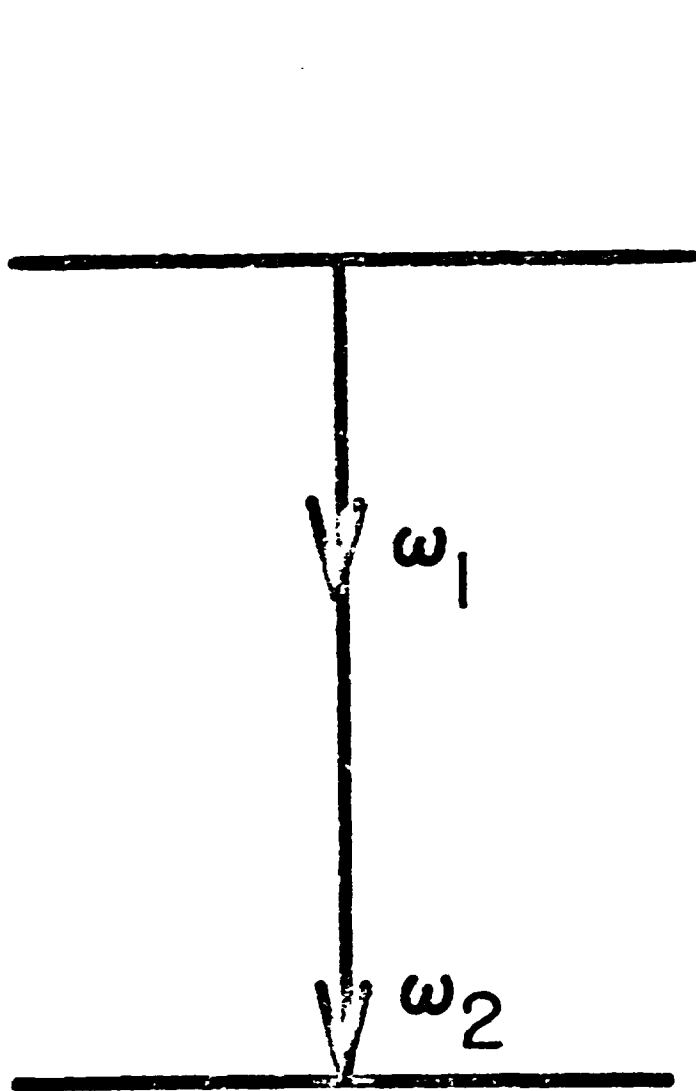
AN EXAMPLE OF LASER BEAM ARRAY OF ARRAYS



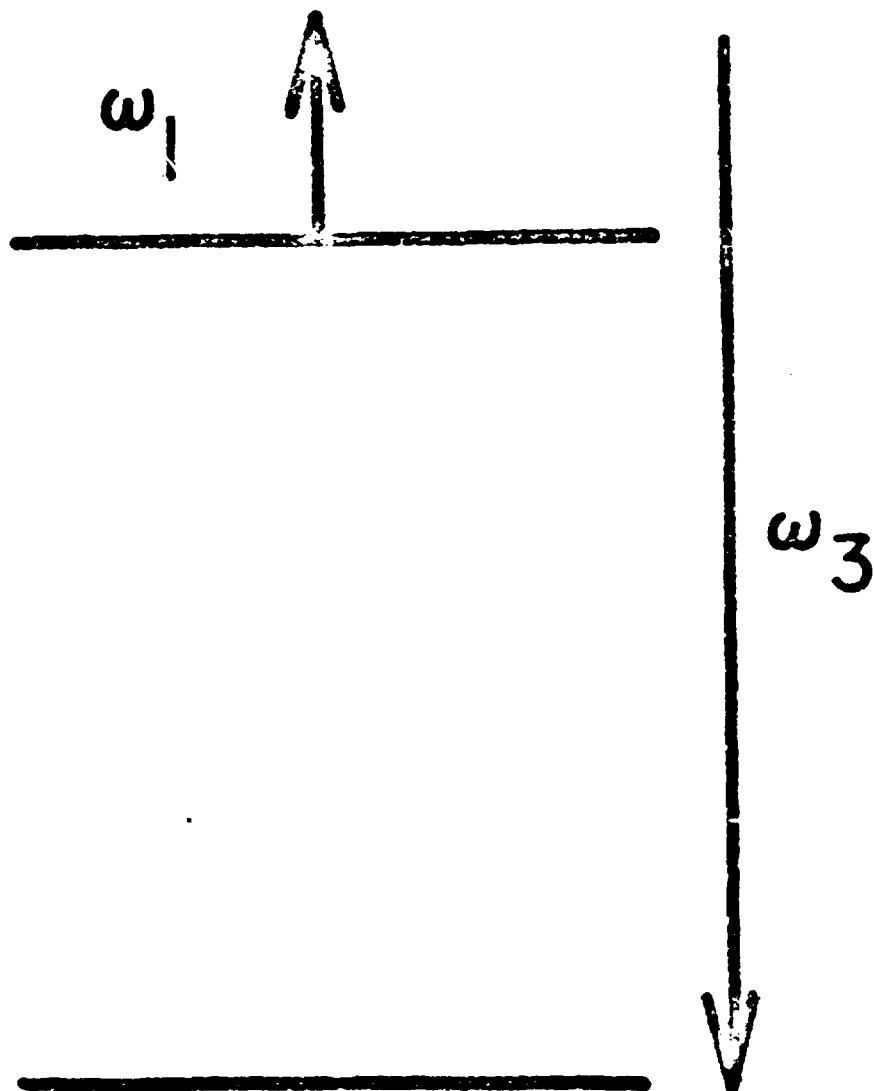






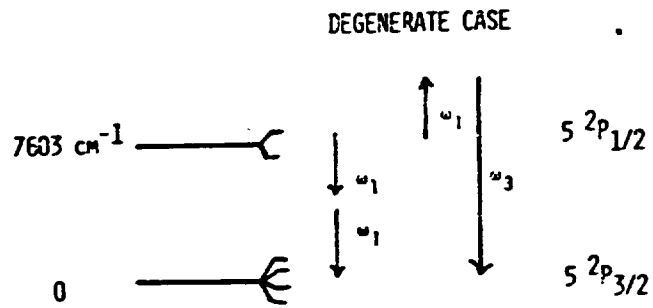
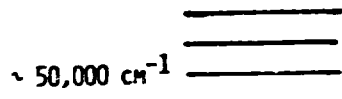


(A)

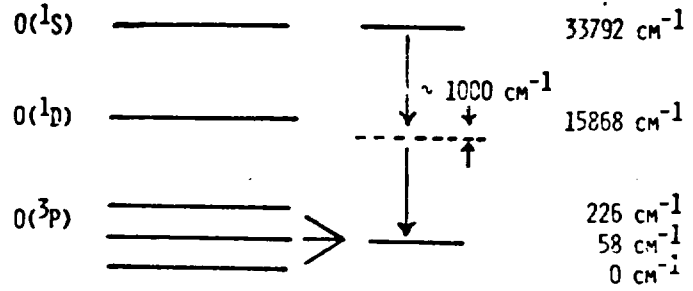


(B)

RELEVANT ATOMIC IODINE SPECTROSCOPY



RELEVANT ATOMIC OXYGEN SPECTROSCOPY

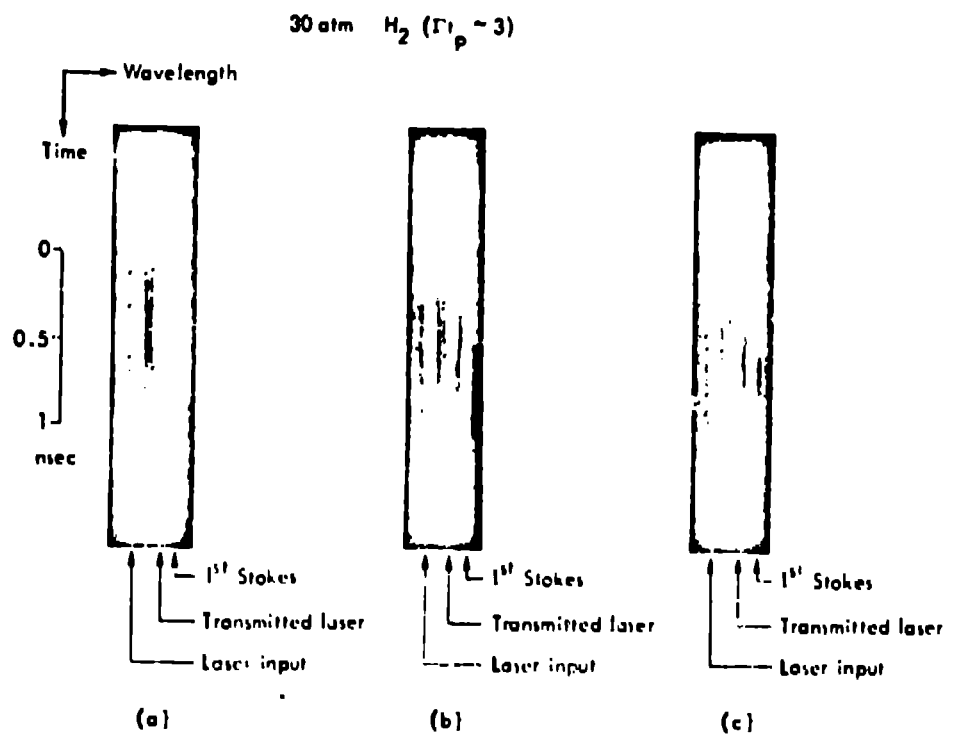
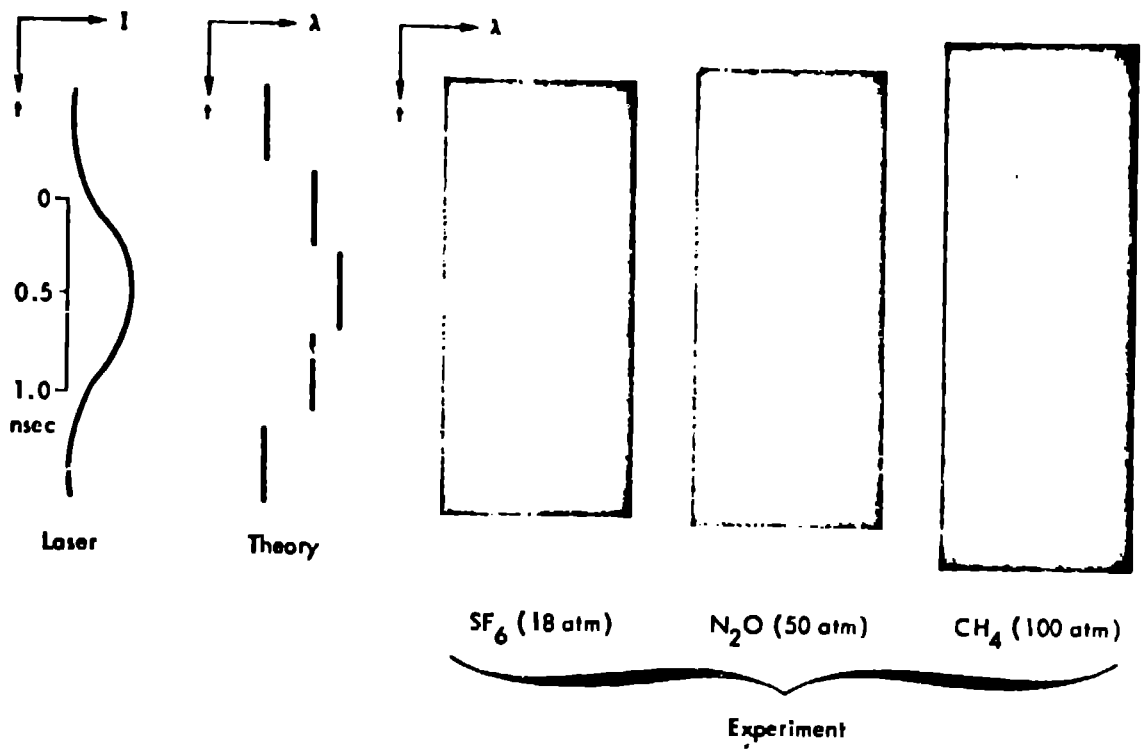


$1S \text{ TO } 1D \quad \sigma_{\text{DOPPLER}} = 9 \times 10^{-19} \text{ cm}^2$

Fig 8.
R. I. Cannon

A

B



TWO-PHOTON AMPLIFIER EXPERIMENT IN ATOMIC IODINE

